Glucose Oxidase Embedded ZnO Nanowires/Ferrocenyl-Alkanethiol Array for efficient glucose-sensing application

Bairui Tao[1, 2], Rui Miao[1], Wenyi Wu[1], Fengjuan Miao[1*]*

[1] College of Communications and Electronics Engineering, Qiqihar University, Heilongjiang 161006, China
[2] Modern Education Technology Center, Qiqihar University, Heilongjiang 161006, China
[*] E-mail: tbr_sir@163.com; miaofengjuan@163.com

One-dimensional ZnO nanowires/ferrocenyl-alkanethiol array is synthesized on silicon substrate combined by self-assembled and low temperature aqueous methods. Electro-catalytic responses of glucose oxidase/ ZnO nanowires/ferrocenyl-alkanethiol array/Silicon (GOx/ZnO NWs/FcC11SH/Si) electrode are detected deeply. The ZnO nanowires/ferrocenyl-alkanethiol array has provided a favorable environment to the immobilization of glucose oxidase. The morphology and crystal structure of the as-grown products have been characterized by many methods, including scanning electron microscopy (SEM), X-ray diffraction (XRD) and electrochemical test. Electrochemical results demonstrated that the well configuration GO_x/ZnO NWs/FcC11SH/Si possessed excellent electrocatalytic activity to glucose, which provide a meaningful way for the practical applications in clinical, environmental, and food analysis.

1. INTRODUCTION

Accurate and quickly determination of glucose concentration is very important owning to the increase in the number of diabetes patients. Thus more and more researches have been focused on the development of the glucose sensor with good sensitivity and stability as well as fast response time. Enzyme-based electrochemical glucose biosensors are based on reactions catalyzed by enzymes, has been extensively studied due to their high sensitivity, excellent selectivity and low cost features [1-3]. One of the major issues when working with enzymes is their stability [4], that is, the maintenance of their activity. Many efforts have been made on this issue, and appropriate matrix for the immobilization of enzymes is one of the best solutions.

As an important Ⅱ-Ⅵ group semiconductor, ZnO has numerous potential applications, such as used in gas sensors and actuators, solar cells, and transistors and so on [5-7]. Especially, ZnO show great promise on electrochemical application due to their many special characteristics, such as high adaptability, good stability, and so on, which make it suitable for absorption of proteins. Glucose oxidase (GOx) has the low IEP (~4.2), which enables GOx to be combined with ZnO in phosphate buffer solution (PBS) with PH 7.4 by electrostatic interaction [8-10]. These properties produce ZnO nanostructure promising in the application of glucose biosensor. To date, different kinds of ZnO nanostructures have been used to fabricate different kind of enzymatic biosensors, especially, one-dimensional ZnO nanomaterials ranging from needles, rods, belts, tubes, wires, used more popular for immobilized for glucose oxidase owning to their high aspect ratio[11-14]. However, the absence of redox centers in ZnO is causing a hindrance toward the performance of glucose sensor. So more and more researches get more efforts to find a middle layers to introduce certain extrinsic redox species and then fabricate an effective path for electrons transfer between enzyme to the electrode.

11-ferrocenyl-1-undecanethiol ($FcC_{11}SH$) is a good redox mediator, which could enhance the rate of electronic communication through generated a large redox current. Many groups have employed it to fabricated biosensor [15, 16]. As we known, there has few reports ever mentioned it application on glucose biosensor with one-dimensional ZnO nanomaterials based on silicon substrate.

In this article, the $FcC_{11}SH$ layer was first synthesized by self-assembled on silicon substrate with coated a thin Au film, and then ZnO nanowires were fabricated by low temperature aqueous method. The as-prepared ZnO NWs/FcC11SH/Si nanocomposites were characterized by XRD, SEM and PL. The ZnO nanowires have a well defined configuration with about 1000 nm in length. A glucose biosensor was fabricated using ZnO NWs/FcC11SH/Si as supporting materials. The biosensor shows high sensitivity for glucose detection.

2. EXPERIMENTAL DETAILS

2.1 Substrates and reagents

Analytical-grade zinc acetate dehydrate [Zn $(CH_3COO)_2 \cdot 2H_2O$], sodium sulfate, 11-ferrocenyl-1-undecanethiol ($FcC_{11}SH$), Ethanolamine (C_2H_7NO), Ethanolamine (C_2H_7NO), ammonia hydroxide ($NH_3 \cdot H_2O$), and ethanol were used as-received without further purification. Single-polished (100) silicon wafers were used as the substrates.

2.2 Preparation of substrates and Self-assembling of FcC_{11}SH

Firstly, silicon wafers with thickness of ~500 μm were cleaned and pre-etched in order to remove contaminations and surface oxides. Then, the silicon wafers were deeply cleaned by a hot Paraha solution ($H_2SO_4:H_2O_2=3:1$ in volume) for 15 minutes, Next, these silicon wafers were cut into rectangles with needed dimensions. Secondly, a 30 nm Ti layer and 100 nm Au layer was deposited on the surface of silicon by thermal evaporation, respectively. Thirdly, the as-prepared substrates were

immersed in a 10 mM ethanol solution of FcC11SH for 24 h. After self-assembling, the electrode was rinsed with ethanol and deionized water several times. Lastly, the modified substrate was kept in a 0.1 M sodium sulfate solution at 4 °C for use.

2.2 Synthesis of ZnO NWs/FcC$_{11}$SH/Si array

ZnO seed layers were prepared by spin coating and then annealed at 350 °C for 30 min in ambient air for growth the NWs arrays.

ZnO NWs arrays were synthesized based on the seeded by using the hydrothermal method. In a typical synthesis process, Zn (CH$_3$COO)$_2$·2H$_2$O, NH$_3$·H$_2$O were mixed in distilled water with a well stirred. Then put the above substrate with ZnO seed layer in this reaction solution for 2 h at 80 °C. After the preparation, the samples was cleaned with distilled water and dried under argon to stabilize the structure. The ZnO NWs/FcC$_{11}$SH/Si array grown on silicon substrate was then characterized by different instruments.

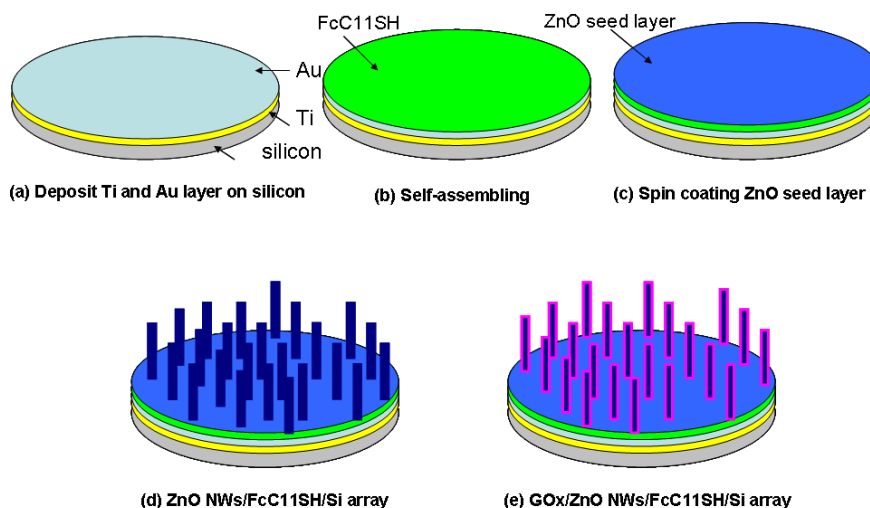## 2.3 Immobilization of GOx in the whole structures

Figure 1. The schematic diagram of the GOx/ZnO NWs/FcC11SH/Si array fabrication process.

The biosensor was fabricated by immobilizing glucose oxidaseon on the surface of as prepared ZnO NWs/FcC$_{11}$SH/Si array through electrostatic interaction, in which a thin Nafion film was used to assisted natural adsorption.

The GOx and nafion was mixed in 0.01 M PBS and then dropped on the surface of the ZnO NWs/FcC$_{11}$SH/Si array. Then the whole structure was washed repeatedly with deionized water to remove the unimmobilized GOx, finally the sample was kept at 2-4 °C overnight for further use, and the electrode was stored in PBS at 4 °C when not in use. The fabrication process of the GO$_x$/ZnO NWs/FcC$_{11}$SH/Si array is shown in Fig1.

2.4 Characterization

The morphology and structure of the prepared ZnO NWs/FcC$_{11}$SH/Si arrays were characterized by many methods, such as scanning electron microscopy (SEM), atomic force microscopy (AFM) , and X-ray diffractometer (XRD) with Cu Ka radiation (λ = 0.15405nm) with the instrument resolution ~0.02° steps in 2θ. All the electrochemical experiments were carried out in a conventional three-electrode cell controlled by electrochemical workstation.   All the experiments were performed at around 25 °C.

3. RESULTS AND DISCUSSION

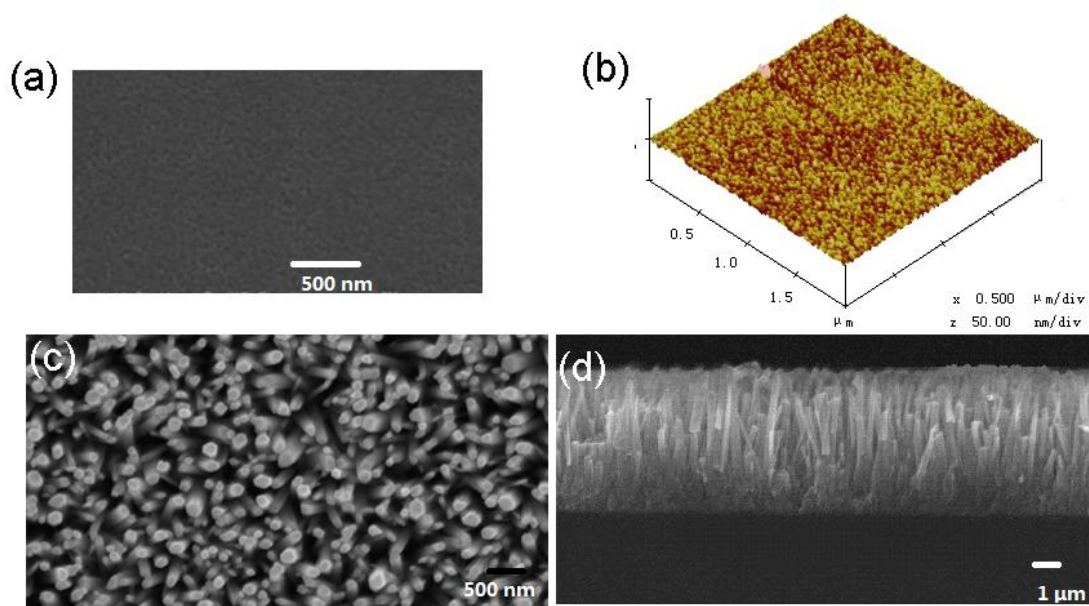*3.1. Characterization of the ZnO NWs/FcC$_{11}$SH/Si arrays electrode*

Figure 2. (a): Top-view SEM image of the ZnO seed layers; (b): AFM micrographs of the ZnO seed layers, (c) Top-view SEM image of the ZnO nanowires, and (d) Cross-sectional SEM image of the ZnO nanowires.

Fig.2 (a) and Fig.2 (b) show the SEM and AFM micrographs of the ZnO seed layers synthesis on the FcC$_{11}$SH/Si substrate, respectively. It is obviously that the surface of the film is composed of closely packed ZnO nanoparticles whose sizes are in the range of 40-80 nm. The three-dimensional AFM image shows the surface of the seed layers is relatively smooth. Fig.2(c) and Fig.2 (d) illustrate the top and cross-sectional SEM images of the ZnO nanowires grown on the FcC$_{11}$SH coated silicon substrates by hydrothermal method. It can be seen that the ZnO nanowires are vertically grown on the FcC$_{11}$SH/Si substrate, and the average diameter of ZnO nanowires are about 80 nm, the average length of the ZnO nanowires are about 1000 nm. It is obviously, this nanostructure has high aspect ratio.
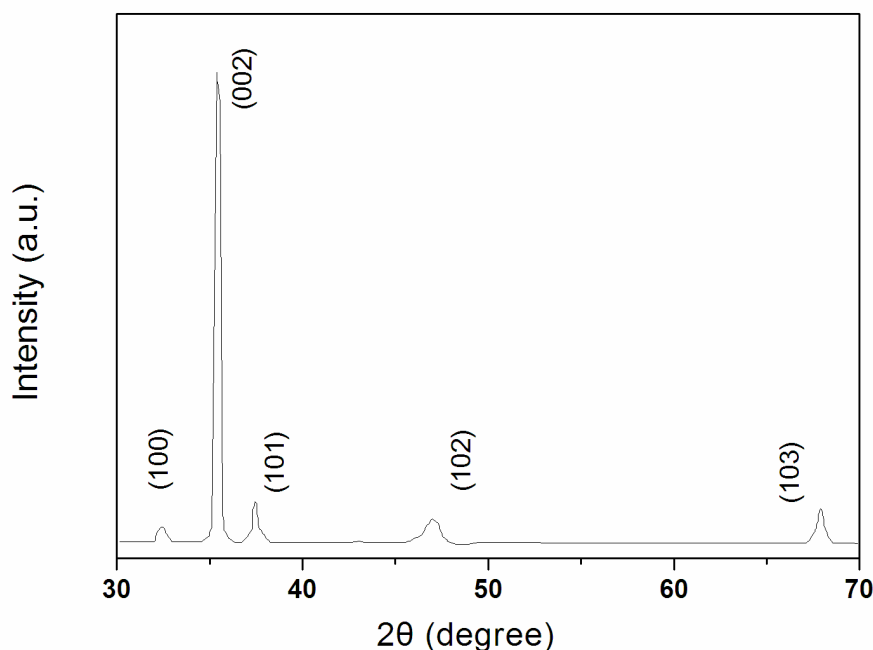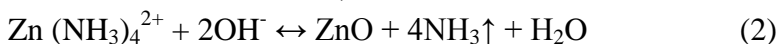
Figure 3. The XRD results of the ZnO NWs/FcC11SH/Si nanostructure.

Fig.3 shows the XRD results of the ZnO NWs/FcC$_{11}$SH/Si nanosructure. The diffraction spectrum shows a (002) peak with relatively strong intensities. It is also detected other diffraction peaks with a much lower intensity mainly at 2θ = 31.71 °, 36.21 °, 47.51 °, 56.61 ° and 62.8 ° appear in XRD spectrum. These diffraction peaks can be assigned to the reflections from the (100), (101), (102), (110), and (103) of ZnO [17]. The diffractions spectrum indicates that the crystalline structure of ZnO has been formed.

3.2. Formation mechanism of the ZnO NWs/FcC$_{11}$SH/Si arrays electrode

The growth mechanism of ZnO NWs suggested above can be expressed as Eq. (1-2) [18-20]:
$$Zn^{2+} + 4NH_3 \cdot H_2O \leftrightarrow Zn\,(NH_3)_4^{2+} + 4H_2O \qquad (1)$$
$$Zn\,(NH_3)_4^{2+} + 2OH^- \leftrightarrow ZnO + 4NH_3\uparrow + H_2O \qquad (2)$$
The growth of ZnO NWs is a pure chemical solution process, and the solid-liquid interface had little influence on the whole growth process of the ZnO nanorods. So in our growth process, the combination between the ZnO NWs and the substrates is the physisorption such as is governed by the free surface energy, etc.

3.3 Electrocatalytic activity of Nafion/GOx/ZnO NWs/FcC$_{11}$SH/Si nanosructure electrode

The electro-catalytic activities of the sensing electrode were studied in 0.01 M PBS (PH7.4) with and without glucose.
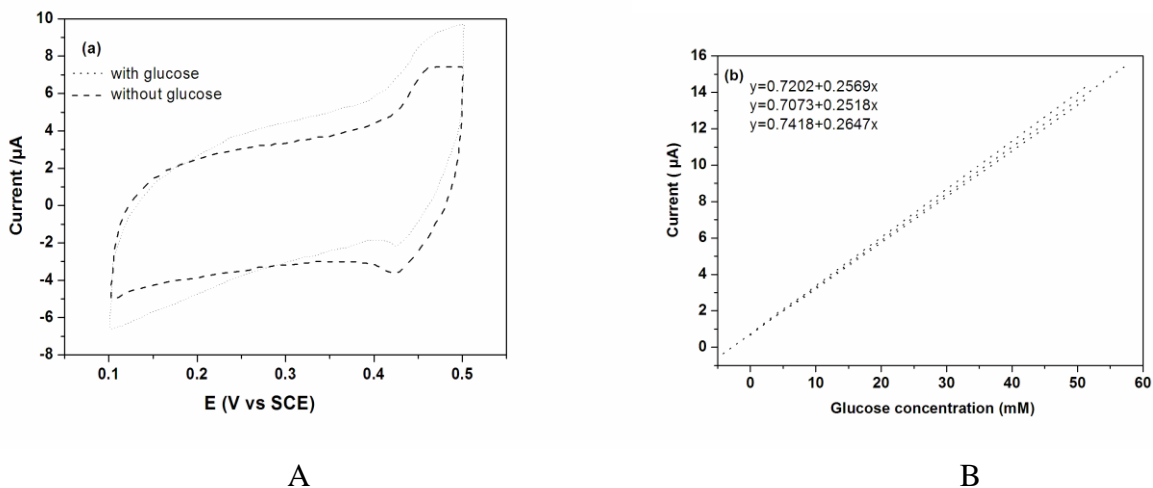
Figure 4. (a): Cyclic voltammetric sweep curves for the Nafion/GOx/ZnONWs/FcC11SH/Si electrode in 0.01 M PBS solution present and absent 1 mM glucose, respectively; (b) Cyclic voltammetric sweep curves for the Nafion/GOx/FcC11SH/Si electrode in 0.01 M PBS solution present and absent 1 mM glucose, respectively;

Fig.4 shows cyclic voltammetric sweep curves for the Nafion/GOx/ZnONWs/FcC$_{11}$SH/Si electrode (Fig.4 (a)) and Nafion/GOx/FcC$_{11}$SH/Si electrode (Fig.4 (b)) in 0.01 M PBS solution present and absent 1 mM glucose, respectively. The CV results show an increased oxidation current density after added glucose for both Nafion/GOx/ZnONWs/FcC$_{11}$SH/Si and Nafion/GOx/FcC$_{11}$SH/Si electrode, which indicating that the GOx is very sensitive to the glucose solution. At the same times, there were tiny changes on the central locations of the redox peak-to-peak that reveals the electron transfer between FcC$_{11}$SH and Si are stable, and the existence of FcC$_{11}$SH molecular can introduce a shutting way for electronic communication between GOx and electrode.
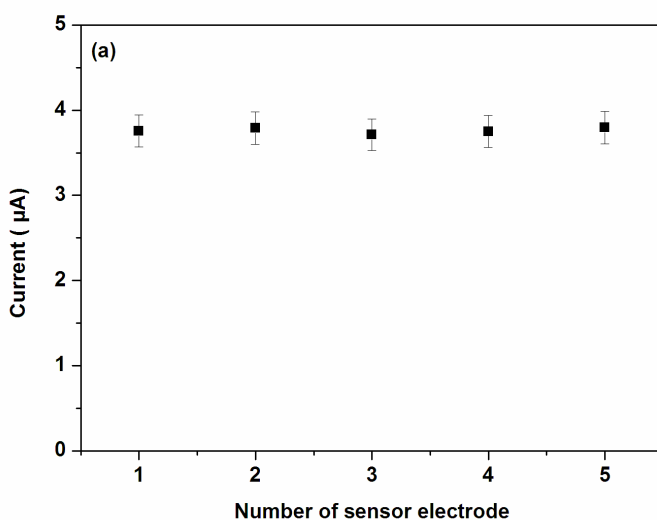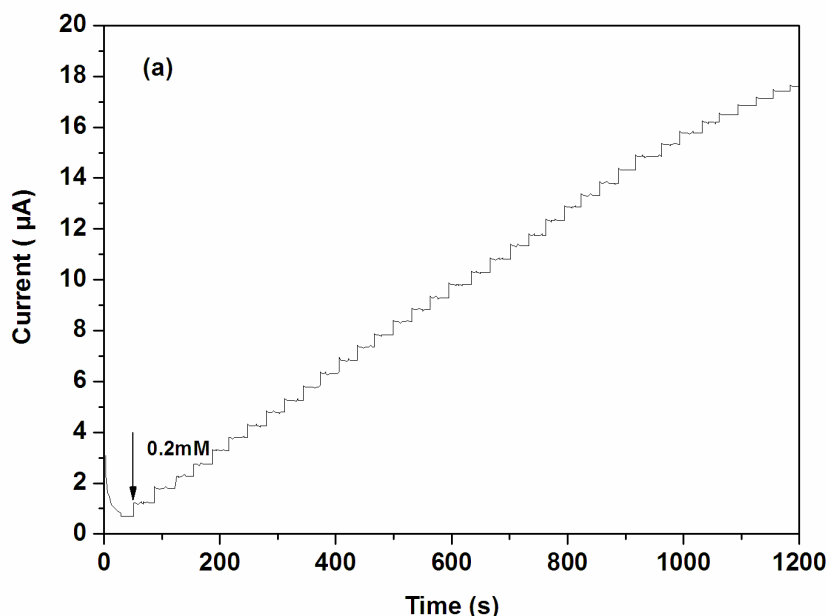
B

Figure 5. (a): The amperometric response performance of the biosensor; (b): The plot of the current density versus glucose concentration.

It is evidently that the current density of Nafion/GOx/ZnONWs/FcC$_{11}$SH/Si electrode higher than Nafion/GOx/FcC$_{11}$SH/Si electrode is due to ZnO nanowires support high surface to area ratio for immobilization of GOx, which increased the loading content in unit areas.

The amperometric response performance of the biosensor was calculated by testing the Nafion/GOx/ZnONWs/FcC$_{11}$SH/Si electrode in PBS with successive addition of glucose under stirring. With each addition of glucose, oxidation current of the prepared electrode exhibited a visible increase and achieved 95% stable value in an average of 4 s (Fig.5(a)). This phenomenons demonstrated that the fabricated biosensor was sensitive response to the change of glucose concentration. From the above results, the relationship between the current density and the glucose concentration was shown in Fig.5 (b). It can be seen that the linear detection range of the biosensor is 0.2-5.4 mM with a correction coefficient R=0.9995 and the sensitivity calculated from the calibration curve (Fig. 5(b)) is 35.6 μA mM^{-1}. Furthermore, an extremely low detection limit of 11 μM at a signal-to-noise of 3 (S/N=3) could be obtained, which owning to the fast electron conduction between fixed GOx and the ZnO nanowires.

The enzymic affinity of the whole nanostructured electrode is very importance to the sensitivity. We could calculate the apparent Michaelis-Menten constant K_M^{app} value using Lineweaver-Burk plots to obtain the enzymic affinity in the fabricated electrode. The electrochemical enzymetric process could be exhibited by Eq. (3):
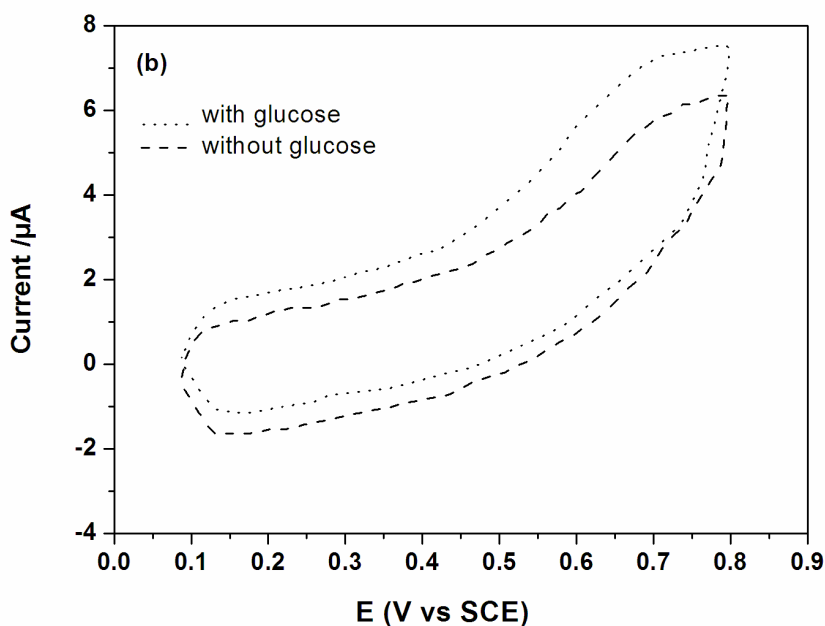
$$\frac{1}{i} = \frac{K_M^{app}}{i_{max}} \left[\frac{1}{C} \right] + \frac{1}{i_{max}} \qquad\qquad (3)$$

Where i , i_{max} and C are the current, the maximum current and the glucose concentration, respectively. The lowest value of K_M^{app} corresponds to the high affinity of ZnO nanowires to GOx. The result calculated is 3.67 mM, showing high affinity of the GOx in the biosensor to glucose.
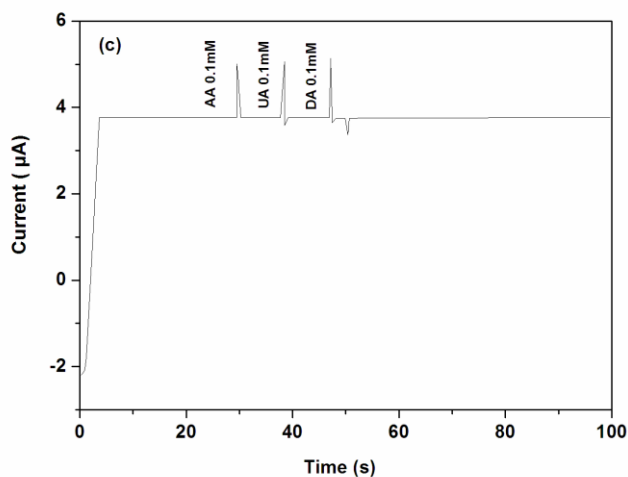
3.4 Reproducibility, Stability, and anti-Interference studies
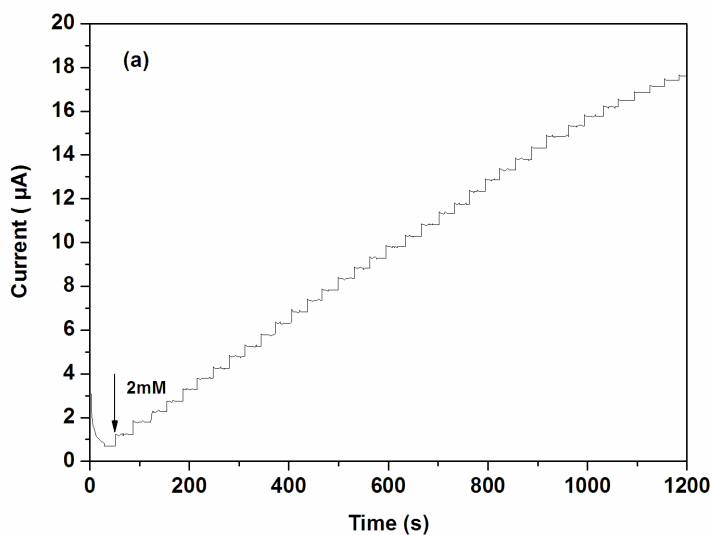
A

B

C

Figure 6. Reproducibility (a), stabilityand (b) and anti-Interference (c) of the glucose-sensing Nafion/GOx/ZnONWs/FcC$_{11}$SH/Si electrodes.

Fig.6 (a) shows a reproducibility test of 5 independently developed Nafion/GOx/ZnONWs/FcC$_{11}$SH/Si electrodes in 0.01 M PBS solution with 1 mM glucose. The relative standard deviation determined was less than 6%. Fig.6 (b) displays the results of three experiments of the same glucose-sensing. Nanocomposite electrode shows good repeatability. The nanocomposite electrode was carefully washed with deionized water after each measurement to clean and remove the residual ions from the surface of the electrode. It is well-known that uric acid (UA), ascorbic acid (AA) and dopamine (DA) are common interfering species during catalytic oxidation of glucose. Thus, we conducted the interference test by measuring currents changes caused by addition of UA, AA and DA during glucose sensing. The results are shown in Fig.6(c) and shows that the addition of these materials did not substantially change the signal. Additional of 0.1 mM UA, 0.1 mM AA, and 0.1 mM DA of UA, AA and DA only generated some small transient signals. This result illustrates that GOx has good selectivity to glucose, and the interfering substances have no obvious effects on the performance of the modified electrode, which will also be attributed to the well maintained activity of enzymes, that is, the as-prepared ZnONWs/FcC$_{11}$SH/Si nanostructure is an ideal platform for enzymes [21-22].

Table 1. A comparison of basic parameters for glucose sensors

Working electrode	sensitivity	Detection limit	Linear range	References
ZnO nanotubes	0.6 μA mM^{-1}	44 μM	0.04-5 mM	[25]
ZnO nanorods	1.02 μA mM^{-1}	19 μM	0.019-7 mM	[24]
Nafion/GOx/ZnO/SiNWs	129 μA mM^{-1}	12 μM	0-25 mM	[23]
Nafion/GOx/ZnONWs/FcC11SH/Si	35.6 μA mM^{-1}	11 μM	0.2-5.4 mM	This work

A performance comparison of our work with other glucose sensors is summarized in Table1. The excellent performance of the Nafion/GOx/ZnONWs/FcC11SH/Si electrode results from the framework with high specific surface area, abundant microspaces which are favorable for the immobilization of enzymes, and the shutting way for electronic communication between GOx and electrode byFcC11SH molecular.

4. CONCLUSION

In summary, ZnONWs/FcC$_{11}$SH/Si nanostructure was synthesized via a simple method both through self-assembled and low temperature aqueous. The as-synthesized ZnONWs/FcC$_{11}$SH/Si nanostructure was used to immobilize GOx and shows better performance to glucose oxidation, due to the high specific surface area, abundant microspaces which are favorable for the immobilization of enzymes, and the shutting way for electronic communication between GOx and electrode byFcC$_{11}$SH molecular. The sensor exhibit very strong and sensitive current responses to glucose even in the presence of high concentrations of interfering species, in addition to showing excellent long-term stability and good reproducibility.

References

1. M.M. Rahman, A.J. Saleh Ahammad, J. Jin, S.J. Ahn, J. Lee, *Sensors*, 10 (2010) 4855.
2. Z.X. Shen, W.Y. Gao, et al. *Talanta*, 159 (2016) 194.
3. L.X. Fang, B. Liu, L.L. Liu, Y.H. Li, K.J. Huang, Q.Y. Zhang, *Sensors and Actuators B: Chemical*, 222 (2016) 1096.
4. D. Grieshaber, R. MacKenzie, J. Vörös, E. Reimhult, *Sensors,* 8 (2008) 1400.
5. F.Y. Huang, Y.M. Zhong, J. Chen, S.X. Li, Y.C. Li, F. Wang, S.Q. Feng, *Analytical Methods*, 5 (2013) 3050.
6. S.W. Kim, S. Fujita, *Applied Physics Letters*, 81, (2002) 5036.
7. L.Q. Liu, K.Q. Hong, X. Ge, D.M. Liu, M.X. Xu, *Journal of Physical Chemistry C*, 118 (2014) 15551.
8. E. Topoglidis, E. Palomares, Y. Astuti, A. Green, C. J. Campbell and J. R. Durrant, *Electroanalysis*, 17 (2005)1035.
9. J. X. Wang, X. W. Sun, A. Wei, Y. Lei, X. P. Cai, C. M. Li and Z. L. Dong, *Appl. Phys. Lett.*, 88 (2006) 233106.
10. A. Wei, X. W. Sun, J. X. Wang, Y. Lei, X. P. Cai, C. M. Li, Z. L. Dong and W. Huang, *Appl. Phys. Lett.*, 89(2006) 123902.
11. D. Ledwith, S.C. Pillai, G.W. Watson, J.M. Kelly, *ChemCommun.* 20 (2004) 2294.
12. Z. Yang, Q.H. Liu, L. Yang, *Materials Research Bulletin*, 42 (2007) 221.
13. Z.W. Pan, Z.R. Dai, Z.L. Wang, *Science,* 291 (2001) 1947.
14. L. Vayssieres, K. Keis, A. Hagfeldt, S.E. Lindquist, *Chem Mater*, 13 (2001) 4395.
15. M.E. Ghica, C.M.A. Bret, *Analytical Letters*, 38 (2005) 907.
16. Y. Peng, C.W. Wei, Y.N. Liu, J. Li, *Analyst,*136 (2011) 4003.

17. Y.M. Huang, Q.L. Ma, B.G. Zhai, *Mater. Lett*. 93 (2013) 266.
18. L.S. Wang, D. Tsan, B. Stoeber, K. Walus, *Adv. Mater.* 24 (2012) 3999.
19. S. Danwittayakul, J. Dutta, *Journal of Alloys and Compounds*, 586 (2014) 169.
20. Z. Wang, X.F. Qian, J. Yin, Z.K. Zhu, *Langmuir*, 20 (2004) 3441.
21. F. Zhou, W.X. Jing, Q. Wu, W.Z. Gao, Z.D. Jiang, J.F. Shi, Q.B. Cui, *Materials Science in Semiconductor Processing*, 56 (2016) 137.
22. K. Tian, S. Alex, G. Siegel, A. Tiwari, *Materials Science and Engineering: C*, 46 (2015) 548.
23. F.J. Miao, X.X. Lu, B.R. Tao, R. Li, P. K. Chu, Microelectronic Engineering, 149 (2016) 153.
24. W. X. Jing, F. Zhou, W. Z. Gao, Z. D. Jiang, W. Ren, J. F. Shi, Y. Y. Cheng and K. Gao, RSC Advances, 5 (2015) 85988.
25. F, Zhou, W.X. Jing, Q. Wu, W.Z. Gao, Z.D. Jiang, J.F.Shi, Q.B. Cui, Materials Science in Semiconductor Processing, 56 (2016) 137.